Bounded positive control for double-pipe heat exchangers

A. Zavala-Río [a,*], C.M. Astorga-Zaragoza [b]
O. Hernández-González [b]

[a] *Instituto Potosino de Investigación Científica y Tecnológica*
Apdo. Postal 2-66, Lomas 4a. Sec. 78216, San Luis Potosí, S.L.P., Mexico

[b] *Centro Nacional de Investigación y Desarrollo Tecnológico*
Int. Internado Palmira, Palmira, C.P. 62490, Cuernavaca, Mor., Mexico

Abstract

In this work, an outlet temperature control scheme for double-pipe heat exchangers is proposed. Compared to previously proposed approaches, the algorithm developed here takes into account and actually exploits the analytical and stability properties inherent to the open-loop dynamics. As a result, outlet temperature regulation is achieved through a simple controller which does not need to feed back the whole state vector and does not depend on the exact value of the process parameters. Moreover, the proposed approach guarantees positivity and boundedness of the input flow rate without entailing a complex control algorithm. The analytical developments are corroborated through simulation and experimental results.

Key words: Double-pipe heat exchangers; temperature control; global regulation; bounded positive input; saturation

1 Introduction

Because of their numerous applications in industrial processes, heat exchangers have been the subject of many studies including, among others: steady-state, transient, and frequency response analysis (Abdelghani-Idrissi and Bagui 2002, Abdelghani-Idrissi *et al.* 2002, Bartecki 2007); open-loop qualitative behavior characterization (Zavala-Río and Santiesteban-Cos 2007, Zavala-Río *et al.* 2003); numerical simulation (Papastratos *et al.* 1993, Zeghal *et al.* 1991);

---

* Correspoding author. Tel.: +52–444–834.7213, fax: +52–444–834.2010.
  Email address: `azavala@ipicyt.edu.mx` (A. Zavala-Río).

state reconstruction (Astorga-Zaragoza *et al.* 2007, Bagui *et al.* 2004); parameter identification (Chantre *et al.* 1994, Ghiaus *et al.* 2007); fault diagnosis/detection (Persin and Tovornik 2005, Loparo *et al.* 1991); and feedback control (Alsop and Edgar 1989, Malleswararao and Chidambaram 1992, Katayama *et al.* 1990, Lim and Ling 1989, Ramírez *et al.* 2004, Gude *et al.* 2005, Maidi *et al.* 2008, Wellenreuther *et al.* 2006). Among these topics, the lastly mentioned one has played an important role in the solution formulation to cope with the operation conditions imposed to current industrial processes. In particular, unexpected behaviors that deteriorate the closed-loop performance and/or prevent the pre-specified convergence goal are undesirable or unacceptable. Thus, a control scheme prepared to avoid such unexpected or undesirable phenomena is always preferable.

Control of heat exchangers has been developed in the literature through the application of several techniques. For instance, based on a simple compartmental model, partial and total linearizing feedback algorithms have been proposed in (Alsop and Edgar 1989) and (Malleswararao and Chidambaram 1992). Unfortunately, such techniques compensate for the system dynamics, neglecting its analytical and stability natural properties. This gives rise to complex control algorithms that depend on the exact knowledge of the system model structure and parameters, and on the accurate measurement of all the process states.

Other works, like that in (Katayama *et al.* 1990), which proposes an optimal control scheme, or that in (Lim and Ling 1989), where a generalized predictive control algorithm is developed, make use of ARX, ARMAX, or ARIMAX type models. Nevertheless, since these are (numerically) adjusted through the output response to input tests, disregarding the natural laws that determine the process behavior, such approaches also neglect the analytical and stability natural properties of the system. Besides, the efficiency of such control methods is highly dependent on an accurate parameter identification of the involved models. Moreover, the estimations resulting from the performed identification method could differ among the regions of the system state-space domain (in view of the linear-discrete character of such models in contrast with the actual nature of the system dynamics).

More recently, a min-max model predictive control scheme was applied to a heat exchanger in (Ramírez *et al.* 2004). Nevertheless, such a design methodology generally gives rise to control algorithms that suffer a large computation burden due to the numerical min-max problem that has to be solved at every sampling time. The use of hinging hyperplanes reduced this disadvantage in (Ramírez *et al.* 2004), but complicated the controller design procedure. Furthermore, works like that in (Gude *et al.* 2005), where conventional P, PI, and PID algorithms were tested, that in (Maidi *et al.* 2008) where a PI fuzzy controller was proposed, or that in (Wellenreuther *et al.* 2006), where a

multi-loop controller tuned using game theory was considered, lack of formal stability proofs and/or stability region estimations.

On the other hand, as far as the authors are aware, previous works on control design for double-pipe heat exchangers do not simultaneously consider the positive (unidirectional) and bounded nature of the flow rate taken as input variable. Such controllers could eventually try to force the actuators to go beyond their natural capabilities, undergoing the well-known phenomenon of saturation. In a general context, the presence of such a nonlinearity is not necessarily disadvantageous as long as it is taken into account in the control design and/or the closed loop analysis. Otherwise, it may give rise to undesirable effects as pointed out for instance in (Slotine and Li 1991, §5.2). Thus, control design considering those input constraints turns out to be important in order to avoid such unexpected or undesirable closed-loop system behaviors.

In this work, a simple control scheme for the process (hot) fluid outlet temperature regulation of double-pipe heat exchangers is proposed, taking the cold fluid (coolant) flow rate as control input. The proposed algorithm takes into account the analytical and stability natural properties of the exchanger, as well as the positive and bounded nature of the flow rate taken as input variable. The resulting controller does not depend on the exact knowledge of the system parameters, does not need to feed back all the process states, and guarantees stabilization to the desired outlet temperature for any initial condition within the system state-space domain. The analytical developments are corroborated through simulation and experimental results.

The text is organized as follows. In Section 2, the nomenclature, notation, and preliminaries that support the developments are stated. Section 3 presents the standing assumptions as well as the system dynamics and some of its analytical properties. In Section 4, the proposed controller is presented and the closed-loop stability analysis is developed. Simulation and experimental results are shown in Section 5. Finally, conclusions are given in Section 6.

2 Nomenclature and notation

Throughout the paper, the system variables and parameters are denoted as follows:

F mass flow rate [kg/s]
C_p specific heat [J/(°C · kg)]
M total mass inside the tube [kg]
U overall heat transfer coefficient [J/(°C · m^2 · s)]
A heat transfer surface area [m^2]
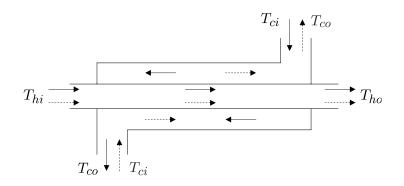
Fig. 1. Counter/parallel-flow (full/dashed arrows resp.) double-pipe heat exchanger

T	temperature [°C]
t	time [s]
ΔT	temperature difference [°C]
$\mathbb{R}$	set of real numbers
$\mathbb{R}_+$	set of positive real numbers
$\mathbb{R}^n$	set of n-tuples (x_j) with $x_j \in \mathbb{R}$
$\mathbf{0_n}$	origin of $\mathbb{R}^n$
$\mathbb{R}_+^n$	set of n-tuples (x_j) with $x_j \in \mathbb{R}_+$

Subscripts:

u	upper bound	l	lower bound
c	cold	h	hot
i	inlet	o	outlet

Let ΔT_1 and ΔT_2 stand for the temperature difference at each terminal side of the heat exchanger, *i.e.*

$$\Delta T_1 \triangleq \begin{cases} T_{hi} - T_{co} & \text{if } \alpha = 1 \\ T_{hi} - T_{ci} & \text{if } \alpha = -1 \end{cases} \quad \text{and} \quad \Delta T_2 \triangleq \begin{cases} T_{ho} - T_{ci} & \text{if } \alpha = 1 \\ T_{ho} - T_{co} & \text{if } \alpha = -1 \end{cases}$$

where

$$\alpha \triangleq \begin{cases} 1 & \text{if counter flow} \\ -1 & \text{if parallel flow} \end{cases}$$

see Fig. 1. The *logarithmic mean temperature difference* (LMTD) among the fluids is typically expressed as (see for instance (Zavala-Río *et al.* 2005) and references therein):

$$\Delta T_\ell \triangleq \frac{\Delta T_2 - \Delta T_1}{\ln \frac{\Delta T_2}{\Delta T_1}}$$

Nonetheless, this expression reduces to an indeterminate form when $\Delta T_1 = \Delta T_2$, which is specially problematic in the counter flow case. Such an indeter-

4

mination is avoided if the LMTD is taken as

$$\Delta T_L \triangleq \begin{cases} \Delta T_\ell & \text{if } \Delta T_2 \neq \Delta T_1 \\ \Delta T_0 & \text{if } \Delta T_2 = \Delta T_1 = \Delta T_0 \end{cases} \tag{1}$$

This was proved in (Zavala-Río *et al.* 2005), together with the following analytical properties.

Lemma 1 (Lemma 2 and Remark 3 in (Zavala-Río *et al.* 2005)) ΔT_L in Eq. (1) is continuously differentiable at every $(\Delta T_1, \Delta T_2) \in \mathbb{R}_+^2$. Moreover, it is positive on $\mathbb{R}_+^2$, while $\lim_{\Delta T_1 \to 0} \Delta T_L = 0$ for any $\Delta T_2 \in \mathbb{R}_+$, and $\lim_{\Delta T_2 \to 0} \Delta T_L = 0$ for any $\Delta T_1 \in \mathbb{R}_+$. ◁

Lemma 2 (Zavala-Río *et al.* 2005, Lemma 3) ΔT_L in Eq. (1) is strictly increasing in its arguments, *i.e.* $\frac{\partial \Delta T_L}{\partial \Delta T_i} > 0$, $i = 1, 2$, $\forall (\Delta T_1, \Delta T_2) \in \mathbb{R}_+^2$. ◁

Finally, the interior and boundary of a set, say $\mathcal{B}$, will be respectively denoted as $\text{int}(\mathcal{B})$ and $\partial \mathcal{B}$.

3 The system dynamics

The following assumptions are considered:

A1. The fluid temperatures and velocities are radially uniform.
A2. The overall heat transfer coefficient is axially uniform and constant.
A3. Constant fluid thermophysical properties.
A4. No heat transfer with the surroundings (adiabatic operation).
A5. Fluids are incompressible and single phase.
A6. Negligible axial heat conduction.
A7. There is no energy storage in the walls.
A8. Inlet temperatures, T_{ci} and T_{hi}, are constant.
A9. The flow rates are axially uniform and any variation is considered to take place instantaneously at every point along the whole length of the exchanger.
A10. The hot fluid flow rate, F_h, is kept constant, while the value of the cold fluid flow rate, F_c, can be arbitrarily varied within a compact interval $\mathcal{F}_c \triangleq [F_{cl}, F_{cu}]$, for some positive constants $F_{cl} < F_{cu}$.

Under these assumptions, and taking the whole exchanger as one *bi-compartmental cell*, a suitable lumped-parameter dynamical model for a double-pipe

heat exchanger is (see for instance (Zavala-Río and Santiesteban-Cos 2007)):

$$\dot{T}_{co} = \frac{2}{M_c} \left[F_c \left(T_{ci} - T_{co} \right) + \frac{UA}{C_{pc}} \Delta T_L (T_{co}, T_{ho}) \right] \tag{2a}$$

$$\dot{T}_{ho} = \frac{2}{M_h} \left[F_h \left(T_{hi} - T_{ho} \right) - \frac{UA}{C_{ph}} \Delta T_L (T_{co}, T_{ho}) \right] \tag{2b}$$

where $\Delta T_L(\cdot, \cdot)$ is the LMTD (complemented) expression in Eq. (1), considered a function of (T_{co}, T_{ho}). A physically reasonable state-space domain for the system in Eqs. (2) is

$$\mathcal{D} \triangleq \begin{cases} \{(T_{o1}, T_{o2}) \in \mathbb{R}^2 \mid T_{ci} < T_{oj} < T_{hi}, \; j = 1, 2\} & \text{if } \alpha = 1 \\ \{(T_{o1}, T_{o2}) \in \mathbb{R}^2 \mid T_{ci} < T_{o1} < T_{o2} < T_{hi}\} & \text{if } \alpha = -1 \end{cases}$$

(see for instance (Zavala-Río and Santiesteban-Cos 2007, Zavala-Río *et al.* 2003)).

The control objective consists in the regulation of the process (hot) fluid outlet temperature T_{ho}, towards a (pre-specified) desired value T_{hd}, through the cold fluid flow rate F_c as input variable, taking into account the restricted range and unidirectional nature of such an input flow rate (according to Assumption A10). The use of a simple model, like Eqs. (2), for the control design aiming at the achievement of such an objective is desirable (Masada and Wormley 1982, Xia *et al.* 1991). Indeed, a high order process dynamics representation would end up in a complex scheme with complicated expressions (Alsop and Edgar 1989) and would involve temperature measurements of intermediate points throughout the exchanger which are not always available. In particular, the model in Eqs. (2) has been used for control design for instance in (Alsop and Edgar 1989) and (Malleswararao and Chidambaram 1992). It has actually been used as a suitable dynamics representation of double-pipe heat exchangers for numerous purposes, as pointed out in (Zavala-Río and Santiesteban-Cos 2007).

Remark 1 Notice that by considering ΔT_L a function of (T_{co}, T_{ho}) on $\mathcal{D}$, continuous differentiability and positivity hold for all (T_{co}, T_{ho}) on $\mathcal{D}$, and 0 (zero) may be considered the value that ΔT_L takes at any (T_{co}, T_{ho}) on $\partial\mathcal{D}$ such that $\Delta T_1(T_{co}, T_{ho}) \cdot \Delta T_2(T_{co}, T_{ho}) = 0$ (see Lemma 1 in Section 2). Furthermore, strict monotonicity in its arguments holds as (applying the chain rule): $\frac{\partial \Delta T_L}{\partial T_{ho}} > 0$ and $\frac{\partial \Delta T_L}{\partial T_{co}} < 0$, $\forall (T_{co}, T_{ho}) \in \mathcal{D}$ (see Lemma 2 in Section 2). $\triangleright$

Remark 2 Let $\boldsymbol{y}$ denote the open-loop state vector, *i.e.* $\boldsymbol{y} \triangleq (T_{co}, T_{ho})^T$, and let $\dot{\boldsymbol{y}} = \bar{\boldsymbol{f}}(\boldsymbol{y}; \boldsymbol{\theta})$ represent the open-loop system dynamics in Eqs. (2) assuming constant flow rates, where $\boldsymbol{\theta} \in \mathbb{R}_+^p$ (for some positive integer p) is the system parameter vector. Considering Lemma 1, it can be seen (from Eqs. (2)) that $\bar{\boldsymbol{f}}$ is continuously differentiable in $(\boldsymbol{y}; \boldsymbol{\theta})$ on $\mathcal{D} \times \mathbb{R}_+^p$. Then, the system solutions

$\boldsymbol{y}(t; \boldsymbol{y_0}, \boldsymbol{\theta})$, with $\boldsymbol{y_0} \triangleq \boldsymbol{y}(0) \in \mathcal{D}$, do not only exist and are unique, but are also continuously differentiable with respect to initial conditions and parameters, for all $\boldsymbol{y_0} \in \mathcal{D}$ and all $\boldsymbol{\theta}$ sufficiently close to any nominal parameter vector $\boldsymbol{\theta_0} \in \mathbb{R}_+^p$ (see for instance (Khalil 1996, §2.4)). $\qquad \triangleright$

In (Zavala-Río and Santiesteban-Cos 2007), it was shown that, considering constant flow rates, the system dynamical model in Eqs. (2) possesses a unique equilibrium point $(T_{co}^*, T_{ho}^*) \in \mathcal{D}$, where

$$
\begin{pmatrix} T_{co}^* \\ T_{ho}^* \end{pmatrix} = \begin{pmatrix} 1 - P & P \\ RP & 1 - RP \end{pmatrix} \begin{pmatrix} T_{ci} \\ T_{hi} \end{pmatrix} \triangleq \begin{pmatrix} g_c(F_c) \\ g_h(F_c) \end{pmatrix} \tag{3}
$$

with $R = \frac{F_c C_{pc}}{F_h C_{ph}}$,

$$
P = \begin{cases} \dfrac{1-S}{1+(-S)^\beta R} & \text{if } R - \alpha \neq 0 \\[4mm] \dfrac{UA}{UA + F_c C_{pc}} & \text{if } R = \alpha = 1 \end{cases}
$$

$S = \exp\left(\frac{\alpha UA}{F_h C_{ph}} - \frac{UA}{F_c C_{pc}} \right)$, and $\beta \triangleq \frac{\alpha+1}{2}$.

Claim 1 g_h *in Eq.* (3) *is a one-to-one strictly decreasing continuously differentiable function of* F_c.

Proof. See Appendix A.1. $\qquad \qquad \square$

Remark 3 Observe that through Claim 1, two important facts are concluded: 1) T_{ho}^* is restricted to a *reachable steady-state space* defined by

$$
\mathcal{R}_h \triangleq [g_h(F_{cu}), g_h(F_{cl})]
$$

2) Any value of $T_{ho}^* \in \mathcal{R}_h$ is uniquely defined by a specific flow rate value $F_c^* \in \mathcal{F}_c$ (Assumption A10), which in turn defines a unique value of T_{co}^* according to Eq. (3). $\qquad \triangleright$

4   The proposed controller

The analysis developed in (Zavala-Río and Santiesteban-Cos 2007), considering constant flow rates, showed that the vector field in Eqs. (2) has a normal component pointing to the interior of $\mathcal{D}$ at every point on $\partial \mathcal{D}$. Consequently, for all initial state vectors in $\mathcal{D}$, the system trajectories remain in $\mathcal{D}$ globally in

time, and are bounded since $\mathcal{D}$ is bounded. Moreover, $\mathcal{D}$ was proven to contain a sole invariant composed by a unique equilibrium point (T_{co}^*, T_{ho}^*). Therefore, every trajectory of the dynamical model in Eqs. (2) converges to (T_{co}^*, T_{ho}^*). The idea is then to propose a dynamic controller such that the closed-loop dynamics keeps the same analytical features, with F_c forced to evolve within $\text{int}(\mathcal{F}_c)$, and forcing the existence of a sole invariant composed by a unique equilibrium point $(T_{co}^*, T_{ho}^*, F_c^*)$ where $T_{ho}^* = T_{hd}$, the (pre-specified) desired value (according to the control objective, stated in Section 3). This is achieved through the following control scheme.

Proposition 1 *Consider the dynamical system in Eqs. (2) with $F_c \in \mathcal{F}_c$. Let the value of F_c be dynamically computed as follows*

$$\dot{F}_c = k\eta(F_c)\,(T_{ho} - T_{hd}) \tag{4}$$

for any $T_{hd} \in \text{int}(\mathcal{R}_h)$, where

$$\eta(F_c) \triangleq (F_c - F_{cl})(F_{cu} - F_c)$$

and k is a sufficiently small positive constant. Then, for any initial closed-loop (extended) state vector $(T_{co}, T_{ho}, F_c)(0) \in \mathcal{D} \times \text{int}(\mathcal{F}_c)$: $T_{ho}(t) \to T_{hd}$ as $t \to \infty$, with $F_c(t) \in \text{int}(\mathcal{F}_c)$, $\forall t \geq 0$, and $\left(T_{co}, T_{ho}\right)(t) \in \mathcal{D}$, $\forall t \geq 0$. ◁

Proof. See Appendix A.2. □

Remark 4 Observe that the proposed approach does not need to feed back the whole extended state vector. No measurements of T_{co} are required for its implementation. Furthermore, the exact knowledge of the accurate values of the system parameters is not needed. Such features characterize the proposed algorithm as a simple controller that gives rise to a control signal evolving within its physical limits. This way, undesirable phenomena, such as *wind-up*, are avoided. ▷

Remark 5 Notice, from the proof of Proposition 1, that inequality (A.1), *i.e.* $k \leq \frac{8F_h C_{ph}(F_{cl}M_h + F_h M_c)}{M_h M_c C_{pc}(F_{cu} - F_{cl})^2(T_{hi} - T_{ci})}$, may be taken as an *a priori* control gain tuning criterion. The right-hand-side expression may be calculated using available system parameter (average) estimations; one may trust that a value of k quite smaller than the calculated bound would satisfy inequality (A.1). Further, one could in general expect that upper and lower bound reliable estimations of each parameter are available, *e.g.* $C_{ph} \in [C_{phl}, C_{phu}]$, $C_{pc} \in [C_{pcl}, C_{pcu}]$, $M_h \in [M_{hl}, M_{hu}]$, $M_c \in [M_{cl}, M_{cu}]$, $F_h \in [F_{hl}, F_{hu}]$ (the inlet temperatures are assumed to be measurable); then by choosing $k \leq \frac{8F_{hl}C_{phl}(F_{cl}M_{hl} + F_{hl}M_{cl})}{M_{hu}M_{cu}C_{pcu}(F_{cu} - F_{cl})^2(T_{hi} - T_{ci})}$, the satisfaction of inequality (A.1) is ensured. Notice, however, that such a condition is not necessary and that it might be conservative. ▷

Remark 6 Observe that the proposed approach may be equivalently expressed as a simple integral action over the error signal $e \triangleq T_{ho} - T_{hd}$ scaled by the non-linear flow-rate-varying gain $\kappa(F_c; k) \triangleq k\eta(F_c)$, *i.e.*

$$F_c(t) = \int_0^t \kappa(F_c(s); k) e(s) ds + F_c(0)$$

Further, each of the involved terms plays an important role in the achievement of the control objective. For instance, the error term, $T_{ho} - T_{hd}$ in Eq. (4), defines the unique closed-loop equilibrium point, $(T_{co}^*, T_{ho}^*, F_c^*)$, naturally locating it such that $T_{ho}^* = T_{hd}$. Notice that this is done without the necessity to *a priori* know the corresponding value of F_c^* and in spite of any eventual modelling inaccuracy. On the other hand, through the non-linear flow-dependent term $\eta(F_c)$ in Eq. (4), the control variable is forced to evolve within its physical limits. Indeed, observe that for any $F_c(0) \in \text{int}(\mathcal{F}_c)$, F_c is not able to go beyond the lower and upper bounds of $\mathcal{F}_c$ since, at F_{cl} or F_{cu}, F_c stops evolving. Moreover, due to the repulsive (unstable) nature of the consequent equilibrium points, $\boldsymbol{x}_l^*$ and $\boldsymbol{x}_u^*$, appearing on the boundary of $\mathcal{D} \times \mathcal{F}_c$, such limit values of F_c, *i.e.* F_{cl} and F_{cu}, cannot even be asymptotically approached. Finally, a sufficiently small control gain, k in Eq. (4), gives rise to a *slowly-varying* input that (slowly) leads $(g_c(F_c), g_h(F_c))$ (see Eq. (3)) towards the desired location. The outlet temperature trajectories (T_{co}, T_{ho}) naturally approach such a *relocating equilibrium point*. The overall phenomena guarantee the global stabilization of the closed-loop system trajectories towards the desired (unique) equilibrium point, whatever initial conditions $(T_{co}, T_{ho}, F_c)(0)$ take place in $\mathcal{D} \times \text{int}(\mathcal{F}_c)$.   ▷

5 Closed loop tests

In order to verify the effectiveness of the proposed controller, experiments were carried out on a bench-scale pilot plant consisting of a completely instrumented double-pipe heat exchanger;[1] see Fig. 2. The plant operates as a water-cooling process —with the hot water flowing through the internal tube and the cooling water flowing through the external pipe— and may be configured in either counter or parallel flow configuration. Engelhard Pyro-Control Pt-100 temperature transmitters measure the temperatures at one extreme of the pipes (the one coinciding with the hot fluid outlet in both flow configurations) while RIY-Moore temperature transmitters measure the temperatures at the other extreme (the one coinciding with the hot fluid inlet in both flow configurations). The current signals produced by the transmitters (in the range

---

[1] A study on the calculation of the system parameters and model validation of such an experimental device (where the dynamical model in Eqs. (2) was validated) has been developed in (Méndez-Ocaña 2006).

Fig. 2. Bench-scale pilot plant

of 4–20 mA) are fed to current-to-voltage converters, and the resulting voltage signals are then read through a data acquisition card (AT-MIO-16E-1 by National Instruments). Both fluid flow rates are measured *via* Platon flowmeters, and the cold fluid flow rate is regulated through a pneumatic valve (Research Control Valve by Badger Meter, Inc.). A monitoring interface, designed using LabVIEW®, displays the controlled output T_{ho} and the manipulated variable F_c.

For the developed experimental tests, the inlet temperatures were kept constant at $T_{ci} = 30\,°\mathrm{C}$ and $T_{hi} = 66\,°\mathrm{C}$. The hot fluid flow rate was fixed at $F_h = 16.7 \times 10^{-3}\,\mathrm{kg/s}$. The cold fluid flow rate F_c was made vary between $F_{cl} = 0.8 \times 10^{-3}\,\mathrm{kg/s}$ and $F_{cu} = 10.8 \times 10^{-3}\,\mathrm{kg/s}$, respectively the lower and upper input bounds.

Closed loop tests were also performed through numerical simulations, taking the same input bounds, hot fluid flow rate, and inlet temperature values of the experimental plant, specified above. The parameters of the simulated exchanger were defined as: $U = 1050\,\mathrm{J/(°C \cdot m^2 \cdot s)}$, $A = 0.014\,\mathrm{m^2}$, $M_c = 0.134\,\mathrm{kg}$, $M_h = 0.015\,\mathrm{kg}$, $C_{pc} = 4174\,\mathrm{J/(°C \cdot kg)}$, and $C_{ph} = 4179\,\mathrm{J/(°C \cdot kg)}$. These were taken from (Astorga-Zaragoza *et al.* 2007) and actually correspond to the estimated (average) parameters of the above-mentioned experimental setup (see Footnote 1). Two modelling cases were simulated: 1) one considering the whole exchanger as a single bi-compartmental cell with Eqs. (2) as dynamic model, and 2) another one considering a 20-bi-compartmental-cell 40th order dynamics, every cell modelled using Eqs. (2), appropriately interconnecting the outlet and inlet temperatures of each compartment to the corresponding contiguous one (see for instance (Alsop and Edgar 1989) or (Weyer *et al.* 2000)).
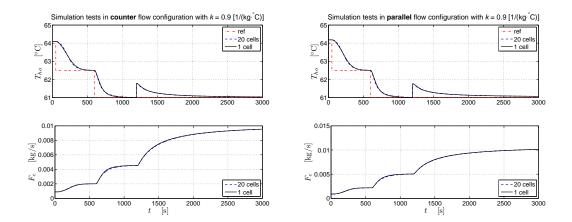
Fig. 3. Simulation results in counter (left) and parallel (right) flow configurations with $k = 0.9\,[1/(°\mathrm{C} \cdot \mathrm{kg})]$

5.1 Simulation results

Numerical tests considering both —counter and parallel— flow configurations were run. In all the performed simulations, the controller gain and the cold fluid flow rate initial value were fixed at $k = 0.9\,[1/(°\mathrm{C} \cdot \mathrm{kg})]$ and $F_c(0) = 0.9 \times 10^{-3}\,\mathrm{kg/s}$. Actually, by assuming that $F_c(t) = 0.9 \times 10^{-3}\,\mathrm{kg/s}$, $\forall t \leq 0$, the exchanger initial temperatures were defined according to the corresponding equilibrium (or *steady-state*) profile (see for instance (Zavala-Río and Santiesteban-Cos 2007)). In particular, $(T_{co}, T_{ho})(0) = (65.16, 64.1)\,[°\mathrm{C}]$ in the counter flow case, and $(T_{co}, T_{ho})(0) = (63.6, 64.19)\,[°\mathrm{C}]$ for the parallel flow configuration. In all the simulated cases, the tests were performed as follows: at $t = 50\,\mathrm{s}$, the loop was closed with $T_{hd} = 62.5\,°\mathrm{C}$; at $t = 600\,\mathrm{s}$, the reference was changed to $T_{hd} = 61\,°\mathrm{C}$; finally, at $t = 1200\,\mathrm{s}$, the hot fluid flow rate was perturbed by changing its value from $F_h = 16.7 \times 10^{-3}\,\mathrm{kg/s}$ to $F_h = 20 \times 10^{-3}\,\mathrm{kg/s}$.

Fig. 3 shows the results of the simulation for both (the counter and the parallel) flow configurations. Note, on the one hand, that practically the same closed-loop performance is achieved in both —the low- and the high-order— modelling cases, with negligible quantitative differences among their responses. Observe, on the other hand, that the control objective is achieved in every case. Notice however that, in both configuration cases, the closed-loop system proved to take longer times to recover from a perturbation than from a reference change. For instance, one sees, from the system responses on the figure, that while a stabilization time of around $300\,\mathrm{s}$ takes place for the reference change produced at $t = 600\,\mathrm{s}$, the system takes more than $1000\,\mathrm{s}$ to recover from the perturbation arisen at $t = 1200\,\mathrm{s}$.

Fig. 4 shows the system responses to the loop closure, with $T_{hd} = 62.5\,°\mathrm{C}$, for different control gains. The same initial conditions of the above-mentioned test
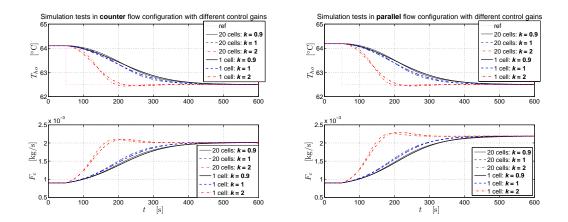
11

Fig. 4. Simulation results in counter (left) and parallel (right) flow configurations with different control gains

were reproduced. Again, note that negligible quantitative differences among the closed-loop responses with the low- and high-order plant models take place. Observe that as the control gain increases, the rising and stabilization times decrease. Notice however that system responses with overshoot are observed in the highest tested control gain case.

5.2 Experimental results

Experiments were carried out in both —counter and parallel— flow configurations. The performed tests were similar to those simulated: the controller gain was fixed at $k = 0.9\,[1/(°\mathrm{C} \cdot \mathrm{kg})]$; the cold fluid flow rate was initially held at $F_c = 2 \times 10^{-3}\,\mathrm{kg/s}$; after *steady-state* temperatures were reached, the experiments were run, holding the initial conditions during $50\,\mathrm{s}$; after such an initial period, the loop was closed with $T_{hd} = 62.5\,°\mathrm{C}$; at $t = 600\,\mathrm{s}$, the reference was changed to $T_{hd} = 61\,°\mathrm{C}$; finally, at $t = 1100\,\mathrm{s}$, the hot fluid flow rate was perturbed by changing its value from $F_h = 16.7 \times 10^{-3}\,\mathrm{kg/s}$ to $F_h = 20 \times 10^{-3}\,\mathrm{kg/s}$.

Fig. 5 shows the experimental results for both (the counter and the parallel) flow configurations. Observe that the control objective is achieved in every case. Further, contrarily to what was predicted through the simulation tests in the precedent subsection, the closed-loop system proves to take comparable times to recover from a perturbation than from a reference change. For instance, one sees, from the graphs on the figure, that a stabilization time of around $200\,\mathrm{s}$ takes place for both the reference change produced at $t = 600\,\mathrm{s}$ and the perturbation arisen at $t = 1100\,\mathrm{s}$.

Fig. 6 shows the experimental system responses to the loop closure, with $T_{hd} = 62.5\,°\mathrm{C}$, for different control gains. The same initial conditions of the
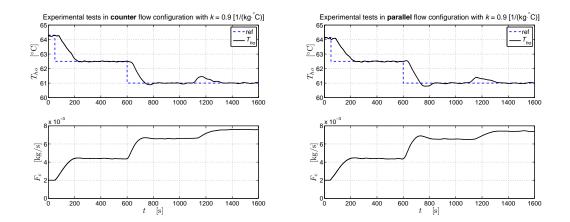
12

Fig. 5. Experimental results in counter (left) and parallel (right) flow configurations with $k = 0.9 \, [1/(^\circ C \cdot \text{kg})]$
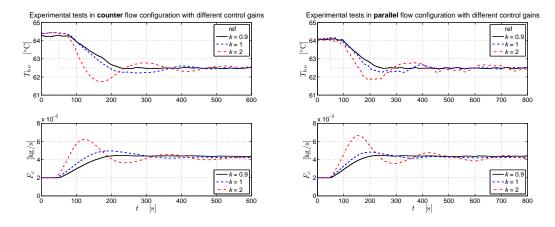

Fig. 6. Experimental results in counter (left) and parallel (right) flow configurations with different control gains

above-described test were reproduced. Observe that as the control gain increases, there is a value above which underdamped system responses arise, and consequently larger stabilization times take place.

For comparison purposes, the linearizing feedback approach developed in (Malleswararao and Chidambaram 1992) was implemented in counter flow configuration. The complete control law, considering the complemented LMTD expression in Eq. (1), is shown in Appendix B; the reader may corroborate the complexity of such a control expression with respect to the simplicity of the algorithm in Proposition 1. The controller parameter values were tuned as suggested in (Malleswararao and Chidambaram 1992) (see Appendix B). In view of the slow closed-loop responses produced by this controller (as will be seen and commented below), two tests were performed. The first test departed from the same initial conditions of the previous experiments, with the cold fluid flow rate initially held at $F_c = 2 \times 10^{-3}$ kg/s; after *steady-state* temperatures were reached, the experiments were run, holding the initial
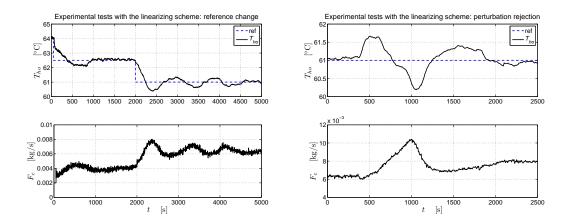
Fig. 7. Experimental results with the linearizing feedback scheme (App. B): reference change (left) and perturbation rejection (right)

conditions during 50 s; after such an initial period, the loop was closed with $T_{hd} = 62.5\,°\text{C}$ and, at $t = 2000$ s, the reference was changed to $T_{hd} = 61\,°\text{C}$. With the system in closed loop, the second test departed from the steady-state conditions produced at the end of the first test; after 360 s, the hot fluid flow rate was perturbed by changing its value from $F_h = 16.7 \times 10^{-3}$ kg/s to $F_h = 20 \times 10^{-3}$ kg/s.

Fig. 7 shows the closed-loop outlet temperature response and control signal arisen with such a linearizing feedback scheme at both performed tests. The results of the first test are shown in the left-hand-side graphs while those of the second test are presented in the right-hand side of the figure. Note that notoriously longer stabilization times take place compared to those previously observed with the proposed scheme. Indeed, note from the graphs on the figures that while a regulation time of about 950 s takes place when the loop was closed (at $t = 50$ s during the first test), the system takes more than 2000 s to get stabilized from the reference change (at $t = 2000$ s during first test) and more than 1500 s to recover from the perturbation (arisen at $t = 360$ s during the second test). Moreover, responses with overshoot are observed during the first test, and oscillating convergence takes place after the reference was changed (during the first test) and when the perturbation was produced (during the second test). Furthermore, observe that the resulting control signals are noisy. This may be a consequence of the high dependence of the linearizing feedback controller on the system states (entailing a high degree of measurement noise corruption).

Further experimental tests were performed implementing a conventional PI controller, *i.e.* $F_c(t) = k_p \left[(T_{ho}(t) - T_{hd}) + \frac{1}{\tau_i} \int_0^t (T_{ho}(s) - T_{hd})ds \right]$, in counter flow configuration. After numerous trial-and-error experimental tests, the control gain combination giving rise to the best closed loop responses was determined to be: $k_p = 1 \times 10^{-3}$ kg/($°\text{C} \cdot$ s) and $\tau_i = 20$ s. With these values, regulation was achieved avoiding oscillations, or giving rise to negligible ones.
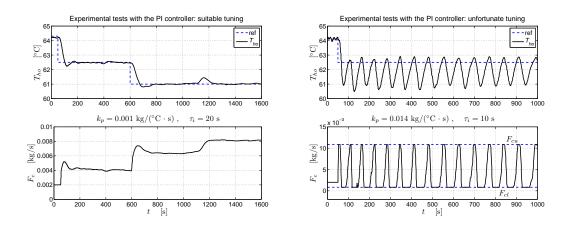
14

Fig. 8. Experimental results under the conventional PI controller with different control parameter tunings: a suitable one (left) and an unfortunate one (right)

Once the controller suitably tuned, a test similar to the one performed for the proposed scheme was reproduced: departing from the same initial conditions, the loop was closed at $t = 50\,\text{s}$ with $T_{hd} = 62.5\,°\text{C}$; at $t = 600\,\text{s}$, the reference was changed to $T_{hd} = 61\,°\text{C}$; and at $t = 1100\,\text{s}$, the hot fluid flow rate was perturbed by changing its value from $F_h = 16.7 \times 10^{-3}\,\text{kg/s}$ to $F_h = 20 \times 10^{-3}\,\text{kg/s}$.

The left-hand-side graphs of Fig. 8 show the closed-loop outlet temperature response and control signal arisen through the experimental implementation of the conventional PI controller with the above-mentioned suitable control parameter value combination. Note that stabilization times comparable to those obtained with the proposed approach took place. In particular, the closed-loop system seems to perform a quicker recovery from the perturbation. Nevertheless, overshoots were observed when the loop was closed at $t = 50\,\text{s}$ and when the reference was changed at $t = 600\,\text{s}$.

The right-hand-side graphs of Fig. 8 show the experimental system responses to the loop closure, with $T_{hd} = 62.5\,°\text{C}$ and departing from the same initial conditions of the above-described test, under the conventional PI control action with a different control parameter value combination, namely: $k_p = 1.4 \times 10^{-2}\,\text{kg/}(°\text{C} \cdot \text{s})$ and $\tau_i = 10\,\text{s}$. Observe from the graphs of the figure that, in this case, a sustained oscillation takes place. Further, the control flow rate sweeps the whole input range several times per period, undergoing lower- and upper-bound input saturation at every cycle. This behavior is due to the unfortunate control parameter tuning, in view of the inherent input saturation levels which are not considered by the controller. Because of the lack of a suitable closed-loop analysis taking into account those input constraints, unfortunate control parameter tunings, that give rise to such type of generally unexpected oscillatory behaviors, may easily be performed.

15

6   Conclusions

In this work, a bounded positive control scheme for the outlet temperature global regulation of double-pipe heat exchangers was proposed. The algorithm guarantees a control signal varying within its physical positive limits, which agrees with the bounded and unidirectional nature of the corresponding flow rate. Moreover, the proposed scheme turns out to be a simple algorithm that does not need to feed back the whole closed-loop state vector and does not depend on the exact knowledge of the system parameters. Numerical simulations and experimental tests corroborated the theoretical developments. Compared to other controllers that were also experimentally implemented, good closed-loop responses were obtained with the proposed algorithm.

A   Proofs

A.1   Proof of Claim 1

Continuous differentiability of g_h with respect to F_c follows from the arguments given in Remark 2. Hence, from Eq. (3), $g_h'(F_c) = \frac{dg_h}{dF_c}(F_c)$ is given by

$$
g_h'(F_c) = \begin{cases} \dfrac{RS\left[1 + \gamma - e^\gamma\right](T_{hi} - T_{ci})}{F_c\left(1 + (-S)^\beta R\right)^2} & \text{if } R - \alpha \neq 0 \\[4mm] -\dfrac{C_{pc}U^2A^2(T_{hi} - T_{ci})}{2C_{ph}F_h\left(UA + C_{ph}F_h\right)^2} & \text{if } R = \alpha = 1 \end{cases}
$$

where $\gamma \triangleq \frac{UA}{C_{pc}F_c} - \frac{\alpha UA}{C_{ph}F_h}$. Thus, from Formula 4.2.30 in [2] (Abramowitz and Stegun 1972), one sees that $g_h'(F_c) < 0$, $\forall F_c > 0$, showing that $g_h(F_c)$ is strictly decreasing on its domain. This, in turn, corroborates its one-to-one character.

A.2   Proof of Proposition 1

Let $\mathcal{T} \triangleq \{T_o \in \mathbb{R} \mid T_{ci} < T_o < T_{hi}\}$, $\boldsymbol{x}$ denote the closed-loop (extended) state vector, i.e. $\boldsymbol{x} \triangleq (T_{co}, T_{ho}, F_c)^T$, and $\dot{\boldsymbol{x}} = \boldsymbol{f}(\boldsymbol{x})$ represent the closed-loop system dynamics. Based on Lemma 1 (see also Remark 1), it can be verified

---

[2] Formula 4.2.30 in (Abramowitz and Stegun 1972) states the following well-known inequality: $e^z > 1 + z$, $\forall z \neq 0$.

that, with $\alpha = 1$:

$$f_1(T_{hi}, T_{ho}, F_c) = \frac{2F_c}{M_c}(T_{ci} - T_{hi}) < 0 \ , \ \ \forall (T_{ho}, F_c) \in \mathcal{T} \times \text{int}(\mathcal{F}_c)$$

$$f_2(T_{co}, T_{ci}, F_c) = \frac{2F_h}{M_h}(T_{hi} - T_{ci}) > 0 \ , \ \ \forall (T_{co}, F_c) \in \mathcal{T} \times \text{int}(\mathcal{F}_c)$$

with $\alpha = -1$:

$$f_1(T_{co}, T_{co}, F_c) = \frac{2F_c}{M_c}(T_{ci} - T_{co}) < 0 \ \ , \ \ \forall (T_{co}, F_c) \in \mathcal{T} \times \text{int}(\mathcal{F}_c)$$

$$f_2(T_{ho}, T_{ho}, F_c) = \frac{2F_h}{M_h}(T_{hi} - T_{ho}) > 0 \ , \ \ \forall (T_{ho}, F_c) \in \mathcal{T} \times \text{int}(\mathcal{F}_c)$$

and for any $\alpha \in \{-1, 1\}$:

$$f_1(T_{ci}, T_{ho}, F_c) = \frac{2UA}{M_c C_{pc}}\Delta T_L(T_{ci}, T_{ho}) > 0 \ \ \ , \ \ \forall (T_{ho}, F_c) \in \mathcal{T} \times \text{int}(\mathcal{F}_c)$$

$$f_2(T_{co}, T_{hi}, F_c) = -\frac{2UA}{M_h C_{ph}}\Delta T_L(T_{co}, T_{hi}) < 0 \ , \ \ \forall (T_{co}, F_c) \in \mathcal{T} \times \text{int}(\mathcal{F}_c)$$

$$f_3(T_{co}, T_{ho}, F_{cl}) = f_3(T_{co}, T_{ho}, F_{cu}) = 0 \ \ \ \ \ , \ \ \forall (T_{co}, T_{ho}) \in \mathcal{D}$$

This shows that there is no point on the boundary of $\mathcal{D} \times \mathcal{F}_c$ where the vector field $\boldsymbol{f}$ has a normal component pointing outwards. Consequently, for any initial extended state vector in $\mathcal{D} \times \text{int}(\mathcal{F}_c)$, the closed-loop system solution cannot leave the system state-space domain $\mathcal{D} \times \text{int}(\mathcal{F}_c)$. Moreover, it is clear that the points on $\partial\mathcal{D} \times \text{int}(\mathcal{F}_c)$ cannot even be approached. On the other hand, from Eq. (4) and Remark 3, it can be easily seen that the closed-loop system has a unique equilibrium point $\boldsymbol{x}^* = (T_{co}^*, T_{ho}^*, F_c^*)$ in $\mathcal{D} \times \text{int}(\mathcal{F}_c)$, where $T_{ho}^* = T_{hd}$ and F_c^* takes the unique value on $\mathcal{F}_c$ through which T_{ho}^* can adopt the desired value T_{hd}. Besides, letting $\boldsymbol{x}_l^* \triangleq \left(g_c(F_{cl}), g_h(F_{cl}), F_{cl} \right)$ and $\boldsymbol{x}_u^* \triangleq \left(g_c(F_{cu}), g_h(F_{cu}), F_{cu} \right)$ (see Eq. (3)), with $g_h(F_{cl}) = \max\{T_{ho}^* \in \mathcal{R}_h\}$ and $g_h(F_{cu}) = \min\{T_{ho}^* \in \mathcal{R}_h\}$ (see Remark 3), it follows that $\boldsymbol{f}(\boldsymbol{x}_l^*) = \boldsymbol{f}(\boldsymbol{x}_u^*) = \boldsymbol{0_3}$. Actually, $\boldsymbol{x}_l^*$ and $\boldsymbol{x}_u^*$ are the only equilibrium points on the boundary of $\mathcal{D} \times \mathcal{F}_c$. The Jacobian matrix of $\boldsymbol{f}$, i.e.

$$\frac{\partial \boldsymbol{f}}{\partial \boldsymbol{x}} = \begin{pmatrix} -\frac{2F_c}{M_c} + \frac{2UA}{M_c C_{pc}}\frac{\partial \Delta T_L}{\partial T_{co}} & \frac{2UA}{M_c C_{pc}}\frac{\partial \Delta T_L}{\partial T_{ho}} & \frac{2(T_{ci} - T_{co})}{M_c} \\ -\frac{2UA}{M_h C_{ph}}\frac{\partial \Delta T_L}{\partial T_{co}} & -\frac{2F_h}{M_h} - \frac{2UA}{M_h C_{ph}}\frac{\partial \Delta T_L}{\partial T_{ho}} & 0 \\ 0 & k\eta(F_c) & k\eta'(F_c)(T_{ho} - T_{hd}) \end{pmatrix}$$

where $\eta'(F_c) = \frac{d\eta}{dF_c}(F_c) = F_{cu} + F_{cl} - 2F_c$, evaluated at $\boldsymbol{x}_l^*$ and $\boldsymbol{x}_u^*$, i.e. $\frac{\partial \boldsymbol{f}}{\partial \boldsymbol{x}}\big|_{\boldsymbol{x}=\boldsymbol{x}_l^*}$ and $\frac{\partial \boldsymbol{f}}{\partial \boldsymbol{x}}\big|_{\boldsymbol{x}=\boldsymbol{x}_u^*}$, have eigenvalues

$$k(F_{cu} - F_{cl})(g_h(F_{cl}) - T_{hd}) > 0$$

17

and

$$k(F_{cl} - F_{cu})(g_h(F_{cu}) - T_{hd}) > 0$$

respectively. Then $\boldsymbol{x}_{\boldsymbol{l}}^*$ and $\boldsymbol{x}_{\boldsymbol{u}}^*$ are repulsive (unstable) and consequently the points on $\mathcal{D} \times \partial \mathcal{F}_c$ cannot be asymptotically approached from the interior of the system state-space domain either. Consequently, for any $\boldsymbol{x_0} \in \mathcal{D} \times \text{int}(\mathcal{F}_c)$, $\boldsymbol{x}(t; \boldsymbol{x_0}) \in \mathcal{D} \times \text{int}(\mathcal{F}_c)$, $\forall t \geq 0$, or equivalently $F_c(t) \in \text{int}(\mathcal{F}_c)$, $\forall t \geq 0$, and $(T_{co}, T_{ho})(t) \in \mathcal{D}$, $\forall t \geq 0$. Now, consider the Jacobian matrix of $\boldsymbol{f}$ at $\boldsymbol{x}^*$, i.e. $\frac{\partial \boldsymbol{f}}{\partial \boldsymbol{x}}\big|_{\boldsymbol{x}=\boldsymbol{x}^*}$. Its characteristic polynomial is given by $P(\lambda) = \lambda^3 + a_2\lambda^2 + a_1\lambda + a_0$, where

$$a_2 \triangleq \left[\frac{2F_c}{M_c} + \frac{2F_h}{M_h} - \frac{2UA}{M_cC_{pc}}\frac{\partial \Delta T_L}{\partial T_{co}} + \frac{2UA}{M_hC_{ph}}\frac{\partial \Delta T_L}{\partial T_{ho}} \right]_{\boldsymbol{x}=\boldsymbol{x}^*}$$

$$a_1 \triangleq \left[\frac{4F_cF_h}{M_cM_h} + \frac{4F_cUA}{M_cM_hC_{ph}}\frac{\partial \Delta T_L}{\partial T_{ho}} - \frac{4F_hUA}{M_hM_cC_{pc}}\frac{\partial \Delta T_L}{\partial T_{co}} \right]_{\boldsymbol{x}=\boldsymbol{x}^*}$$

and $a_0 \triangleq k\bar{a}_0$ with

$$\bar{a}_0 \triangleq \left[\frac{4UA\eta(F_c)(T_{ci} - T_{co})}{M_cM_hC_{ph}}\frac{\partial \Delta T_L}{\partial T_{co}} \right]_{\boldsymbol{x}=\boldsymbol{x}^*}$$

From these expressions and Lemma 2 (see also Remark 1), it can be seen that

$$a_2 > b_2 \triangleq \frac{2F_{cl}}{M_c} + \frac{2F_h}{M_h} > 0$$

$$a_1 > b_1 \triangleq -\frac{4F_hUA}{M_hM_cC_{pc}}\left[\frac{\partial \Delta T_L}{\partial T_{co}} \right]_{\boldsymbol{x}=\boldsymbol{x}^*} > 0$$

$$0 < \bar{a}_0 < \bar{b}_0 \triangleq \frac{4UA\eta\left(\frac{F_{cl}+F_{cu}}{2}\right)(T_{ci} - T_{hi})}{M_cM_hC_{ph}}\left[\frac{\partial \Delta T_L}{\partial T_{co}} \right]_{\boldsymbol{x}=\boldsymbol{x}^*}$$

where the fact that $\eta(F_c) \leq \eta\left(\frac{F_{cl}+F_{cu}}{2}\right)$, $\forall F_c \in \mathcal{F}_c$, has been taken into account. Furthermore, consider that k satisfies

$$k \leq \frac{b_1b_2}{\bar{b}_0} = \frac{8F_hC_{ph}(F_{cl}M_h + F_hM_c)}{M_hM_cC_{pc}(F_{cu} - F_{cl})^2(T_{hi} - T_{ci})} \tag{A.1}$$

Under the satisfaction of this inequality, it turns out that $a_0 = k\bar{a}_0 < k\bar{b}_0 \leq b_1b_2 < a_1a_2$, i.e. $a_0 < a_1a_2$, which is a necessary and sufficient condition for the three roots of $P(\lambda)$ to have negative real part (see for instance Example 6.2 in (Dorf and Bishop 2001)). Thus, $\boldsymbol{x}^*$ is asymptotically stable. Its attractivity is global on $\mathcal{D} \times \text{int}(\mathcal{F}_c)$ if $\{\boldsymbol{x}^*\}$ is the only invariant in $\mathcal{D} \times \text{int}(\mathcal{F}_c)$, which is the case for a small enough value of k. Indeed, from boundedness of $\mathcal{D} \times \text{int}(\mathcal{F}_c)$ and its positive invariance with respect to the closed-loop system dynamics, every solution $\boldsymbol{x}(t; \boldsymbol{x_0} \in \mathcal{D} \times \text{int}(\mathcal{F}_c))$ has a nonempty, compact, and invariant

positive limit set $\mathcal{L}^+$, and $\boldsymbol{x}(t; \boldsymbol{x_0}) \to \mathcal{L}^+$ as $t \to \infty$, $\forall \boldsymbol{x_0} \in \mathcal{D} \times \text{int}(\mathcal{F}_c)$ (see (Khalil 1996, Lemma 3.1)). Then, the global attractivity of $\boldsymbol{x}^*$ on $\mathcal{D} \times \text{int}(\mathcal{F}_c)$ is subject to the absence of periodic orbits on $\mathcal{D} \times \text{int}(\mathcal{F}_c)$ (implying $\mathcal{L}^+ = \{\boldsymbol{x}^*\}$). A sufficiently small value of k renders the closed loop a *slowly varying system* (see (Khalil 1996, §5.7)). Then, the 3rd-order closed-loop dynamics can be approximated by the 2nd-order system in Eqs. (2) with (quasi) constant F_c. Since under such representation no closed orbits can take place,[3] the absence of periodic solutions of the closed-loop (3rd-order) system on $\mathcal{D} \times \text{int}(\mathcal{F}_c)$ is deduced. Thus, in conclusion: $T_{ho}(t) \to T_{hd}$ as $t \to \infty$.

B   Linearizing feedback controller

Under the consideration of the LMTD complemented expression in Eq. (1), the linearizing feedback control scheme developed in (Malleswararao and Chidambaram 1992) for countercurrent heat exchangers is given by

$$F_c = \frac{v - \ddot{T}_{hm} - \frac{2}{M_h}\left(F_h + \frac{UA}{C_{ph}}\frac{\partial \Delta T_L}{\partial T_{ho}}\right)\dot{T}_{ho} - \frac{(2UA)^2}{M_c M_h C_{pc} C_{ph}}\frac{\partial \Delta T_L}{\partial T_{co}}\Delta T_L}{\frac{4UA}{M_c M_h C_{ph}}\frac{\partial \Delta T_L}{\partial T_{co}}(T_{ci} - T_{co})}$$

$$v = -k_p\left[e - \frac{1}{\tau_i}\int_0^t e(s)ds - \tau_d \dot{e}\right]$$

$$e = T_{hm} - T_{ho}$$

T_{hm} is the state of a first order reference model defined as

$$\dot{T}_{hm} = -\lambda_m T_{hm} + \lambda_m T_{hd}$$

for some positive scalar λ_m,

$$\Delta T_L = \begin{cases} \frac{\Delta T_2 - \Delta T_1}{\ln \frac{\Delta T_2}{\Delta T_1}} & \text{if } \Delta T_2 \neq \Delta T_1 \\ \Delta T_0 & \text{if } \Delta T_2 = \Delta T_1 = \Delta T_0 \end{cases}$$

$$\frac{\partial \Delta T_L}{\partial T_{co}} = \begin{cases} \frac{\left[\ln \frac{\Delta T_2}{\Delta T_1} - \frac{\Delta T_2 - \Delta T_1}{\Delta T_1}\right]}{\left[\ln \frac{\Delta T_2}{\Delta T_1}\right]^2} & \text{if } \Delta T_2 \neq \Delta T_1 \\ -\frac{1}{2} & \text{if } \Delta T_2 = \Delta T_1 \end{cases}$$

---

[3] This is verified through Bendixon's Criterion (see for instance (Khalil 1996, Theorem 7.2)), since $\frac{\partial \bar{f}_1}{\partial y_1} + \frac{\partial \bar{f}_2}{\partial y_2} = -a_2 < 0$, $\forall \boldsymbol{y} \in \mathcal{D}$, as was stated and shown in (Zavala-Río and Santiesteban-Cos 2007).

$$\frac{\partial \Delta T_L}{\partial T_{ho}} = \begin{cases} \dfrac{\left[\ln \frac{\Delta T_2}{\Delta T_1} - \frac{\Delta T_2 - \Delta T_1}{\Delta T_2}\right]}{\left[\ln \frac{\Delta T_2}{\Delta T_1}\right]^2} & \text{if } \Delta T_2 \neq \Delta T_1 \\[2em] \frac{1}{2} & \text{if } \Delta T_2 = \Delta T_1 \end{cases}$$

with $\Delta T_1 = T_{hi} - T_{co}$ and $\Delta T_2 = T_{ho} - T_{ci}$. The following tuning criterion is proposed in (Malleswararao and Chidambaram 1992): $k_p = \frac{25}{t_s^2 \xi^2}$, $\tau_i = 0.6 t_s$, and $\tau_d = 0.4 t_s \xi^2$, for some positive constants t_s and ξ. Finally, the following values are suggested in (Malleswararao and Chidambaram 1992) for a good regulatory response: $\lambda_m = 0.05\,[1/s]$, $t_s = 60\,\text{s}$, and $\xi = 0.75$ (these were, consequently, the values taken for the experimental tests in Subsection 5.2).

References

Abdelghani-Idrissi MA, Bagui F. Countercurrent double-pipe heat exchanger subjected to flow-rate step change, Part I: New steady-state formulation. Heat Transfer Engineering 2002; 23:4–11.

Abdelghani-Idrissi MA, Bagui F, Estel L. Countercurrent double-pipe heat exchanger subjected to flow-rate step change, Part II: Analytical and experimental transient response. Heat Transfer Engineering 2002; 23:12–24.

Abramowitz M, Stegun IA. Handbook of mathematical functions. 9th printing. New York: Dover Publications; 1972.

Alsop AW, Edgar TF. Nonlinear heat exchanger control through the use of partially linearized control variables. Chemical Engineering Communications 1989; 75:155–170.

Astorga-Zaragoza CM, Zavala-Río A, Alvarado VM, Méndez RM, Reyes-Reyes J. Performance monitoring of heat exchangers *via* adaptive observers. Measurement 2007; 40:392–405.

Bagui F, Abdelghani-Idrissi MA, Chafouk H. Heat exchanger Kalman filtering with process dynamic acknowledgement. In: Computers and Chemical Engineering 2004; 28:1465–1473.

Bartecki K. Comparison of frequency responses of parallel- and counter-flow type of heat exchanger. In: Proc. 13th IEEE-IFAC International Conference on Methods and Models in Automation and Robotics. 2007. p. 411–416.

Chantre P, Maschke BM, Barthelemy B. Physical modeling and parameter identification of a heat exchanger. In: Proc. 20th International Conference on Industrial Electronics, Control, and Instrumentation. 1994. p. 1965–1970.

Dorf RC, Bishop RH. Modern control systems. 9th ed. Upper Saddle River: Prentice-Hall; 2001.

Ghiaus C, Chicinas A, Inard C. Grey-box identification of air-handling unit elements. Control Engineering Practice 2007; 15:421–433.

Gude JJ, Kahoraho E, Hernández J, Etxaniz J. Automation and control issues applied to a heat exchanter prototype. In: Proc. 10th IEEE Conference on Emerging Technologies and Factory Automation. 2005. p. 507–514.

Katayama T, Itoh T, Ogawa M, Yamamoto H. Optimal tracking control of a heta exchanger with change in load condition. In: Proc. 29th IEEE Conference on Decision and Control. 1990. p. 1584–1589.

Khalil HK. Nonlinear systems. 2nd. ed. Upper Saddle River: Prentice-Hall; 1996.

Lim KW, Ling KV. Generalized predictive control of a heat exchanger. IEEE Control Systems Magazine 1989; 9:9–12.

Loparo KA, Buchner MR, Vasudeva KS. Leak detection in an experimental heat exchanger process: A multiple model approach. IEEE Transactions on Automatic Control 1991; 36:167–177.

Malleswararao YSN, Chidambaram M. Nonlinear controllers for a heat exchanger. Journal of Process Control 1992; 2:17–21.

Maidi A, Diaf M, Corriou JP. Optimal linear PI fuzzy controller design of a heat exchanger. Chemical Engineering and Processing 2008; 47:938–945.

Masada GY, Wormley DN. Evaluation of lumped parameter heat exchanger dynamic models. ASME Paper No. 82-WA/DSC-16; 1982.

Méndez-Ocaña, RM. Adaptive observers for a class of nonlinear systems. M.Sc. Thesis. National Research and Technological Development Center (CENIDET), Mexico; 2006. In spanish.

Papastratos S, Isambert A, Depeyre D. Computerized optimum design and dynamic simulation of heat exchanger networks. Computers and Chemical Engineering 1993; 17:S329–S334.

Persin S, Tovornik B. Real-time implementation of fault diagnosis to a heat exchanger. Control Engineering Practice 2005; 13:1061–1069.

Ramírez, DR, Camacho Ef, Arahal MR. Implementation of min-max MPC using hinging hyperplanes: Application to a heat exchanger. Control Engenieering Practice; 2004; 12:1197–1205.

Slotine JJE, Li W. Applied nonlinear control. Upper Saddle River: Prentice-Hall; 1991.

Wellenreuther A, Gambier A, Badreddin E. Multiloop controller design for a heat exchanger. In: Proc. 2006 IEEE International Conference on Control Applications. 2006. p. 2099–2104.

Weyer E, Szederkéndyi G, Hangos K. Grey box fault detection of heat exchangers. Control Engineering Practice 2000; 8:121–131.

Xia L, de Abreu-Garcia JA, Hartley TT. Modelling and simulation of a heat exchanger. In: Proc. IEEE International Conference on Systems Engineering. 1991. p. 453–456.

Zavala-Río A, Femat R, Romero-Méndez R. Countercurrent double-pipe heat exchangers are a special type of positive systems. In: Benvenuti L, de Santis A, Farina L, editors. Positive Systems. Berlin: Springer; 2003. p. 385–392.

Zavala-Río A, Femat R, Santiesteban-Cos R. An analytical study on the Logarithmic Mean Temperature Difference. Revista Mexicana de Ingeniería Química 2005; 4:201–212. Available at http://www.iqcelaya.itc.mx/rmiq/rmiq.htm

Zavala-Río A, Santiesteban-Cos R. Reliable compartmental models for double-pipe heat exchangers: An analytical study. Applied Mathematical Model 2007; 31:1739–1752.

Zeghal S, Isambert A, Laouilleau P, Boudehen A, Depeyre D. Dynamic simulation: A tool for process analysis. In: Proc. Computer-Oriented Process Engineering, EFChE Working Party. 1991. p. 165–170.

Figure captions

Fig. 1. Counter/parallel-flow (full/dashed arrows resp.) double-pipe heat exchanger

Fig. 2. Bench-scale pilot plant

Fig. 3. Simulation results in counter (left) and parallel (right) flow configurations with $k = 0.9 \left[1/(°\mathrm{C} \cdot \mathrm{kg})\right]$

Fig. 4. Simulation results in counter (left) and parallel (right) flow configurations with different control gains

Fig. 5. Experimental results in counter (left) and parallel (right) flow configurations with $k = 0.9 \left[1/(°\mathrm{C} \cdot \mathrm{kg})\right]$

Fig. 6. Experimental results in counter (left) and parallel (right) flow configurations with different control gains

Fig. 7. Experimental results with the linearizing feedback scheme (App. B): reference change (left) and perturbation rejection (right)

Fig. 8. Experimental results under the conventional PI controller with different control parameter tunings: a suitable one (left) and an unfortunate one (right)